World Academy of Science, Engineering and Technology
International Journal of Biomedical and Biological Engineering
Vol:12, No:8, 2018

MRI Compatible Fresnel Zone Plates made of Polylactic Acid

Daniel Tarrazó-Serrano, Sergio Pérez-López, Sergio Castiñeira-Ibáñez, Pilar Candelas, Constanza Rubio

***Abstract*—**Zone Plates (ZPs) are used in many areas of physics where planar fabrication is advantageous in comparison with conventional curved lenses. There are several types of ZPs, such as the well-known Fresnel ZPs or the more recent Fractal ZPs and Fibonacci ZPs. The material selection of the lens plays a very important role in the beam modulation control. This work presents a comparison between two Fresnel ZP made from different materials in the ultrasound domain: Polylactic Acid (PLA) and brass. PLA is the most common material used in commercial 3D-printers due to its high design flexibility and low cost. Numerical simulations based on Finite Element Method (FEM) and experimental results are shown, and they prove that the focusing capabilities of brass ZPs and PLA ZPs are similar. For this reason, PLA is proposed as a Magnetic Resonance Imaging (MRI) compatible material with great potential for therapeutic ultrasound focusing applications.

***Keywords*—**Fresnel zone plate, magnetic resonance imaging polylactic acid, ultrasound focusing.

I. Introduction

LENSES are widely used in different areas due to its applications. A lens is a device that allows to control propagation, beam forming and focusing the energy that impinges on it. These effects are achieved through the diffractive and refractive capabilities of the lenses. Areas such as food industry [1], pharmaceutical [2], sonochesmitry [3], biomedicine [4], [5] and construction [6] use ultrasounds for different purposes and lenses are useful to focus the energy. In the field of acoustics, lenses are relevant for their multiple applications [7]-[11]. Some examples of the different uses of acoustic lenses can be seen in industry, biomedicine and engineering. Scientists and engineers are currently researching on acoustic lenses and developing new designs and improvements over current ones.

Depending on the application and the type of beam forming, there are different physical phenomena on which the lenses are based. There are acoustic lenses based on the variation of the refractive index that varies through a medium. They are known as Gradient-Index (GRIN) lenses. The variation of the refractive index is achieved by the creation of acoustic labyrinths [12]-[14]. Lenses based on sonic crystals or acoustic resonators have also been developed [15].

The lenses based on the diffractive phenomenon base their behavior on constructive interference on the pressure fields. An example of this type is fractal lenses, capable of generating several foci depending on the type of fractal geometry. There is also Fresnel Zone Plates (FZP). Among the different ways to implement FZPs, the most common and easier is to alternate transparent and blocking zones, which results in a Soret FZP [16]. To obtain these blocking areas, materials that are opaque to sound are required. This is accomplished by selecting those materials that have a high impedance contrast with the host medium. There are studies that have implemented Soret FZP for ultrasounds based on this type of lenses [17].

Acoustic impedance (Z) is defined as the product of the medium density (ρ) and the sound propagation velocity (c) in it. When Soret FZP is used in ultrasounds applications the host medium is usually water. One of the materials that have a high impedance contrast and are highly malleable is brass.

The use of metals in the construction of lenses allows obtaining a high impedance contrast, but limitations arise if they have to be used in fields such as biomedical engineering. These lenses can be used for High Intensity Focused Ultrasounds (HIFU) applications guided by MRI [18].

MRI is a noninvasive technique that uses the phenomenon of nuclear magnetic resonance to obtain information about tissues and organs. It is forbidden to introduce systems not compatible with MRI in the resonance zone. This implies that metallic devices cannot be introduced into the MRI. Therefore, to be able to use lenses that are compatible with MRI, they must be constructed in other materials. One of these materials is the PLA [19].

PLA is a material that has been recently used for the implementation of supports, medical devices and other items for safety in the MRI environment [20]. Its reliability has been demonstrated and given its low construction cost combined with the ability to generate *ad hoc* elements, make of PLA an optimal material that can be used for the construction of acoustic lenses.

In this work the implementation and comparison between Soret FZP lenses made of PLA and brass is proposed. Results

Daniel Tarrazó-Serrano, Sergio Pérez-López and Pilar Candelas are with Centro de Tecnologías Físicas, Universitat Politècnica de València, Camí de Vera s/n, 46022, València, Spain (e-mail: dtarrazo@fis.upv.es, serpelo1@upv.es, pcandelas@fis.upv.es).

Sergio Castiñeira-Ibáñez is with Departamento de Ingeniería Electrónica, Universitat de València, Avd. De la Universitat s/n 46100, Burjassot, València, Spain (e-mail: casiser@uv.es).

Constanza Rubio is with Centro de Tecnologías Físicas, Universitat Politècnica de València, Camí de Vera s/n, 46022, València, Spain (e-mail: crubiom@fis.upv.es).

are obtained and compared both numerically and experimentally. For the experimental results, positioning and acquisition of high-precision data system for ultrasound of the Centro de Tecnologías Físicas has been used. Numerical results have been obtained using the commercial software COMSOL Multiphysics [21].

II. Methodology and Theoretical Analysis

The FZP is structured in concentric circular sections known as Fresnel Regions. Each Fresnel Region makes the same contribution to the focusing procedure. Consecutive Fresnel Regions have a π phase shift between them. The main FZP design parameters to deal with are the Focal Length (F_L), Number of Fresnel Zones (N) and the working frequency (f_0). F_L is defined as the location in the axial coordinate where the acoustic pressure field is focused. N includes both opaque and transparent circular sections. In this work, underwater acoustic transmission is considered. Once the design values have been set, the radial distances (r_n) of the implemented lens can be obtained using (1), which depends on all the previous design parameters and is valid for plane wave incidence.

$$r_n = \sqrt{n\lambda F_L + \left(\frac{n\lambda}{2}\right)} \qquad n = 1,2,\dots,N \tag{1}$$

Nevertheless, these lenses are designed for ultrasound applications where a piston-type source has to be considered. As a result of this condition, FZP lenses that have been implemented on this study have been based on (2).

$$d + F_L + \frac{n\lambda}{2} = \sqrt{d^2 + r_n^2} + \sqrt{F_L^2 + r_n^2} \qquad n = 1,2,\dots,N \tag{2}$$

where d is the separation between the point source and the lens.

TABLE I
Density and Sound Propagation Velocity Values

	Brass	PLA	Water
ρ (kg/m^3)	8400	1240	1000
c (m/s)	4700	2230	1500

In order to evaluate the blocking capacity of the elements of the FZP, the transmission pressure coefficients (t) of the material must be calculated. Accordingly, t is defined as the relation between the transmitted field and the incident field. Given (3), brass and PLA impedances are needed to obtain Z_m values. Hence, sound propagation velocity of the lenses has been characterized in the laboratory by eco-impulse technique. Density values have been provided by the manufacturer data sheets. Impedance values taken for t calculation and numerical modeling are shown in Table I.

$$Z_{in} = Z_m \frac{Z_{out} + jZ_m \tan(k_m d)}{Z_m + jZ_{out} \tan(k_m d)} \tag{3}$$

where k_m is the wavenumber, defined as $k_m = \omega / c_m$. Considering $\omega = 2\pi f_0$. Once Z_{in} is obtained, reflection coefficient is defined in (4).

$$r_{in} = \frac{Z_{in} - Z_{water}}{Z_{in} + Z_{water}} \tag{4}$$

The equation that relates the field balance as a function of the impedances and reflection coefficient of the system is defined in (5) and gives t values depending on the material.

$$|t| = \frac{|p_t^+|}{|p_{in}^+|} = \sqrt{1 - |r_{in}|^2} \tag{5}$$

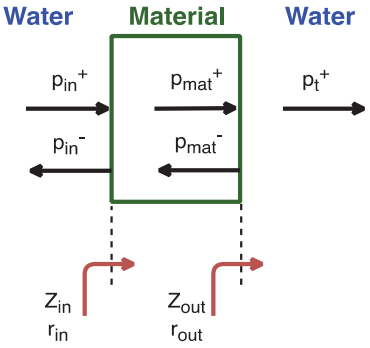

Fig. 1 Transmission diagram of the implemented lenses

The transmission coefficients values obtained using (5) are 0.23 and 0.97 for brass-water and PLA-water, respectively. Bearing in mind these values, it can be affirmed that a full implemented PLA lens will be complex to focus enough energy in the F_L. Therefore, one solution is proposed to obtain the desired impedance contrast. An FZP that includes an air chamber inside the structure has been printed. Thus, both lenses, full-PLA and air-chamber, have been compared.

A. Numerical Models

In order to study the physical phenomena involved in the interaction between the ultrasound waves and the FZPs, it has been necessary to implement a mathematical model that replicates the characteristics of the system. FEM has been used to determine the pressure distribution of the diffracted fields generated by the FZP when there is a piston emitter, causing the interference phenomena. FEM provides an approximate numerical solution of the model [22]. This method performs a discretization of the model and solves the Helmholtz partial differential equation described in (6).

Due to the FZP axisymmetry, the model has been simplified by implementing a semi-lens and applying a rotation with its central axis as the center for its complete generation. This facilitates the reduction of the degrees of freedom necessary to obtain the results of the numerical simulation and thus reducing the calculation time.

In this work, the case of an ideal Soret FZP lens is simulated. In order to model an ideal SZP, rigid blocking elements have been considered. Thus, a comparison between ideal case and experimental models is exposed.

$$\nabla\left(-\frac{1}{\rho}\nabla p\right) = \frac{\omega^2}{\rho c^2} p \tag{6}$$

To solve the Helmholtz equation, typical values of water such as density of the medium (ρ =1000 kg/m^3) and sound

propagation velocity (c=1500 m/s) have been considered. The working frequency of the FZP is 250 kHz and it can be found at (6) by its relation with the angular velocity (ω). Finally, p corresponds to the acoustic pressure.

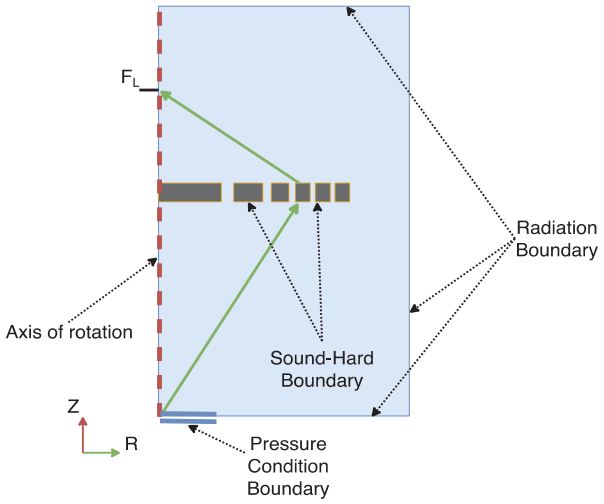

Fig. 2 FEM Scheme of the implemented model simulated on COMSOL Multiphysics

Defined boundary conditions are: the FZP is considered infinitely rigid marking the contours of the elements applying the Newmann condition (the sound velocity in the contour is zero). The contours of the model are defined as wave radiation condition boundary to emulate an infinitely large medium and therefore the Sommerfeld condition is satisfied. The axis of rotation is defined as axis of axisymmetry to simulate the 2π rotation that makes up the FZP in 3D. In Fig. 2, the scheme of the model implemented in FEM is shown.

III. Experimental Set-Up

Lenses have been measured by using an immersion ultrasound high precision system provided by the *Centro de Tecnologías Físicas* at the Universitat Politècnica de València in order to validate and compare the proposed models.

The measurement system is composed by a fixed emitter and a hydrophone coupled to the robotic system. This system obtains reliable and precise results that allow evaluating the acoustic phenomena involved in this type of lenses. As shown in Fig. 3, the lens is immersed in a tank of distilled water.

A plane immersion piston transducer built by Imasonic with 250 kHz of central working frequency and an active diameter of 32 mm has been used as emitter. The hydrophone is a Polyvinylidene fluoride (PVDF) needle transducer (model MPM1/1, Precision Acoustic Ltd.) and has a diameter of 1.5 mm with a flat transfer function between 0.2 and 15 MHz ±4 dB. It has been used as receiver. Acoustic waves emitted by the piston transducer are detected by the needle hydrophone. The pre-amplifier is used to amplify with low noise the hydrophone input signal before it is digitalized by the oscilloscope. This PC oscilloscope is a digital Picoscope Model 3224 from Pico Technology Co. When the data acquired are received by the computer, a time domain averaging with 100 different measurements is realized. The acoustic plane is obtained by automated scanning using steps of 1 x 1 mm^2.

Fig. 3 Picture of the experimental set-up where hydrophone, FZP and piston transducer are shown

IV. Results

The results obtained experimentally and numerically are shown below for 250 kHz. In Fig. 4, lenses implemented in brass and PLA respectively are shown. Both PLA lenses are identical and therefore only one picture of them appears. The difference is that one of them is solid but the other has an inner air chamber.

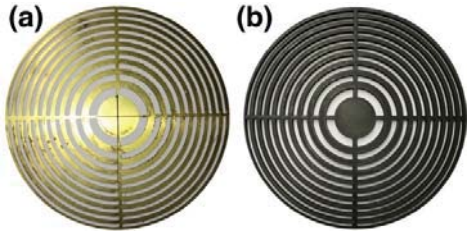

Fig. 4 Implemented FZP lenses. Material used for the construction: (a) Brass, (b) PLA

Intensity gain planes have been calculated to compare all the lenses coherently. These planes are a cut of the RZ axis in the area of interest. Gain (G) is defined as the intensity with lens (I) divided by intensity without lens (I_0) as shown in (7).

$$G(dB) = 10\log_{10}\left(\frac{I}{I_0}\right) \quad (7)$$

In Fig. 5, the gain planes are shown. Focal length designed for the 250 kHz frequency is 50 mm. It can be observed that in the cases of brass and simulated the focus is perfectly located on the F_L. Nevertheless, there is a displacement of 10 mm in the F_L in the PLA with air chamber FZP. This is due to the two PLA interfaces. Resulting from the lack of blocking capability, full PLA FZP could not impede the incident pressure wave transferal generating aberrations in the F_L.

When the blocking capacity of the incident wave is more similar to the design of a Soret FZP lens, non-coherent waves are not introduced allowing better focusing capacity. The ideal case is shown in the numerical solution. The longitudinal and transverse cuts of each one of the cases have been obtained. In Figs. 6 and 7, intensity gain along R and Z axis is presented. The differences among the four cases can be clearly observed.

TABLE II
FWHM AND FLHM VALUES FOR ALL CASES

	FWHM (mm)	FLHM (mm)
Full PLA FZP	2.75	11.0
PLA-Air FZP	3.0	12.8
Brass	3.4	13.0
Simulated	4.0	14.0

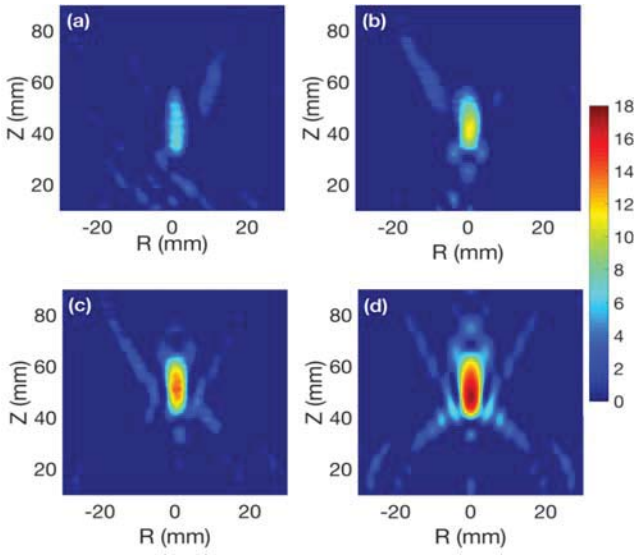

Fig. 5 Intensity Gain map in dB at 250 kHz in RZ plane in mm, (a) Full PLA FZP, (b) PLA with Air chamber FZP, (c) Brass FZP and (d) Simulated FZP

In Table II, a comparison between Full-Width Half Maximum (FWHM) and Full-Length Half Maximum (FLHM) is presented. It can be affirmed that the lower the blocking capacity is, the smaller the focusing capability is. Therefore, the focus depth in both directions is increases with the blocking capability. The gain level discrepancies between the lenses are given by the ratio of the transmission coefficients.

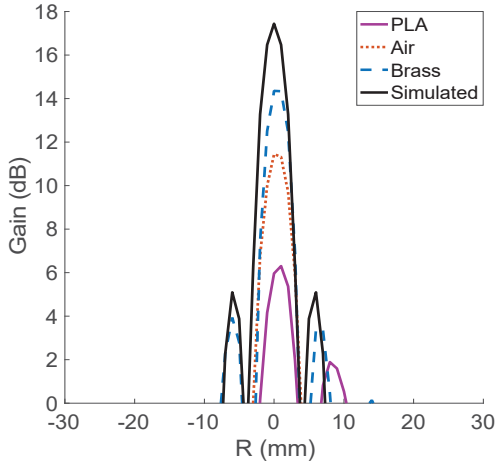

Fig. 6 Intensity Gain along R axis in mm for 4 cases: Full PLA FZP, PLA-Air chamber FZP, brass and simulated

V. CONCLUSION

An alternative way of construction of the FZP lenses that allow compatibility with the MRI has been presented. This type of lens not only allows to obtain the same results as their brass counterparts, but the cost of implementing them is drastically reduced. 3D printers are much more affordable and manageable than numerical control milling units that are required to drill the brass or other metal plates for the construction of the lenses. In addition, the cost of PLA is clearly lower than brass. The spreading of 3D printing technologies means that access to these types of devices will result in cheaper devices.

Using PLA for FZP lenses has benefits in the construction and MRI compatibility of the lens, nonetheless requires an air chamber that allows to reduce the transmission factor to obtain the blocking zones of a Soret FZP. Resulting from the biodegradability of the PLA, microporosities can emerge over time, allowing water to get inside the lens, suppressing the diffraction capabilities, making it transparent to the acoustic waves.

Unfortunately, intensity levels similar to those obtained with a material that generates higher impedance contrast are not achieved. There are other materials compatible with 3D printing systems that could be studied and characterized. Despite of this limitation, this study put forward the use of these materials that allow the use of these lenses in MRI.

ACKNOWLEDGMENT

This work has been supported by TEC2015-70939-R (MINECO/FEDER).

REFERENCES

[1] K. Vilkhu, R. Mawson, L. Simons, and D. Bates, "Applications and opportunities for ultrasound assisted extraction in the food industry—a review," *Innovative Food Science & Emerging Technologies*, vol. 9, no. 2, pp. 161–169, 2008.

[2] S. Albu, E. Joyce, L. Paniwnyk, J. Lorimer, and T. Mason, "Potential for the use of ultrasound in the extraction of antioxidants from rosmar- inus officinalis for the food and pharmaceutical industry," *Ultrasonics Sonochemistry*, vol. 11, no. 3-4, pp. 261–265, 2004.

[3] J.-T. Li, J.-F. Han, J.-H. Yang, and T.-S. Li, "An efficient synthesis of 3, 4-dihydropyrimidin-2-ones catalyzed by nh2so3h under ultrasound irradiation," *Ultrasonics Sonochemistry*, vol. 10, no. 3, pp. 119–122, 2003.

[4] P. Pignoli, E. Tremoli, A. Poli, P. Oreste, and R. Paoletti, "Intimal plus medial thickness of the arterial wall: A direct measurement with ultrasound imaging," *Circulation*, vol. 74, no. 6, pp. 1399–1406, 1986.

[5] R. Illing, J. Kennedy, F. Wu, G. Ter Haar, A. Protheroe, P. Friend, F. Gleeson, D. Cranston, R. Phillips, and M. Middleton, "The safety and feasibility of extracorporeal high-intensity focused ultrasound (hifu) for the treatment of liver and kidney tumours in a western population," *British journal of cancer*, vol. 93, no. 8, p. 890, 2005.

[6] D. McCann and M. Forde, "Review of ndt methods in the assessment of concrete and masonry structures," *NDT and E International*, vol. 34, no. 2, 2001.

[7] D. C. Calvo, A. L. Thangawng, M. Nicholas, and C. N. Layman, "Thin fresnel zone plate lenses for underwater acoustics: Modeling and experiments," *OCEANS'15 MTS/IEEE Washingtonl*, no. October, 2015.

[8] I. Amemiya, H. Yagi, K. Mori, N. Yamamoto, S. Saitoh, C. Tanuma, and S. Hirahara, *Ink Jet Printing with Focused Ultrasonic Beams. Recent Progress in Ink Jet Technologies II*. Society for Imaging Science and Technology, 1999, vol. 5.

[9] S. Hon, K. Kwok, H. Li, and H. Ng, "Self-focused acoustic ejectors for viscous liquids," *Review of scientific instruments*, vol. 81, no. 6, p. 065102, 2010.

[10] Y.-L. Tu, S.-J. Chen, and Y.-R. Hwang, "Design of fresnel lens-type multi-trapping acoustic tweezers," *Sensors*, vol. 16, no. 11, p. 1973, 2016.
[11] E. Schonbrun, C. Rinzler, and K. B. Crozier, "Microfabricated water immersion zone plate optical tweezer," *Applied Physics Letters*, vol. 92, no. 7, p. 071112, 2008.
[12] Y. Li, B. Liang, X. Tao, X. F. Zhu, X. Y. Zou, and J. C. Cheng, "Acoustic focusing by coiling up space," *Applied Physics Letters*, vol. 101, no. 23, 2012.
[13] J. T. Welter, S. Sathish, D. E. Christensen, P. G. Brodrick, J. D. Heebl, and M. R. Cherry, "Focusing of longitudinal ultrasonic waves in air with an aperiodic flat lens," *The Journal of the Acoustical Society of America*, vol. 130, no. 5, pp. 2789–2796, 2011. (Online). Available: http://asa.scitation.org/doi/10.1121/1.3640841.
[14] P. Peng, B. Xiao, and Y. Wu, "Flat acoustic lens by acoustic grating with curled slits," *Physics Letters, Section A: General, Atomic and Solid State Physics*, vol. 378, no. 45, pp. 3389–3392, 2014.
[15] F. Cervera, L. Sanchis, J. V. Sánchez-Pérez, R. Martínez-Sala, C. Rubio, F. Meseguer, C. López, D. Caballero, and J. Sánchez-Dehesa, "Refractive Acoustic Devices for Airborne Sound," *Physical Review Letters*, vol. 88, no. 2, p. 4, 2002.
[16] J. Soret, "Ueber die durch kreisgitter erzeugten diffractionspha¨nomene," *Annalen der Physik*, vol. 232, no. 9, pp. 99–113, 1875.
[17] D. C. Calvo, A. L. Thangawng, M. Nicholas, and C. N. Layman, "Thin Fresnel zone plate lenses for focusing underwater sound," *Applied Physics Letters*, vol. 107, no. 1, 2015.
[18] N. McDannold, K. Hynynen, D. Wolf, G. Wolf, and F. Jolesz, "MRI evaluation of thermal ablation of tumors with focused ultrasound," *Journal of Magnetic Resonance Imaging*, vol. 8, no. 1, pp. 91–100, jan 1998. (Online). Available: http://doi.wiley.com/10.1002/jmri.1880080119.
[19] R. E. Drumright, P. R. Gruber, and D. E. Henton, "Polylactic acid technology," *Advanced Materials*, vol. 12, no. 23, pp. 1841–1846, 2000.
[20] K. H. Herrmann, C. Gärtner, D. Güllmar, M. Krämer, and J. R. Reichenbach, "3D printing of MRI compatible components: Why every MRI research group should have a low-budget 3D printer," *Medical Engineering and Physics*, vol. 36, no. 10, pp. 1373–1380, 2014. (Online). Available: http://dx.doi.org/10.1016/j.medengphy.2014.06.008.
[21] COMSOL Multiphysics, "Comsol multiphysics user guide (version 4.3 a)," *COMSOL, AB*, pp. 39–40, 2012.
[22] O. C. Zienkiewicz, R. L. Taylor, O. C. Zienkiewicz, and R. L. Taylor, *The finite element method*. McGraw-hill London, 1977, vol. 3.